P5.7 A CLIMATOLOGICAL STUDY OF LOW-LEVEL INTERNAL GRAVITY WAVES IN PRECIPITATING ENVIRONMENTS OVER THE KANTO PLAIN, JAPAN

Kenichi Kusunoki *
Meteorological Research Institute, Tsukuba, Japan

1. INTRODUCTION

This paper describes the first climatological study of internal gravity waves, which have horizontal wavelengths of 10km-scale, and propagate horizontally in the lower troposphere in Japan. The coherent gravity wave patterns with significant horizontal wind shear have often been observed in near surface regions far away from the suggested source areas. Therefore, such waves can be extremely hazardous for an aircraft in the takeoff and landing stages of flight. Many properties of these waves such as occurrence, detailed structure, and, environmental conditions are poorly understood due to the lack of comprehensive observations.

In this study, the observations with the Doppler radar for Airport Weather (DRAW) and aircraft soundings of wind and temperature (ACARS) provided unique data of high spatial and temporal resolution, that have been used for analyzing the detailed wave structures.

2. THE STUDY AREA AND DATA SOURCES

The data used in this study include (a) the Narita DRAW data, (b) the Aircraft Communications Addressing and Reporting System (ACARS) data from the surface to a 3000-m height around Narita and Haneda International Airports. The present study focused on the area of the observational range of the Narita DRAW (Figure 1). The area of interest includes the Kanto plain and a part of the Pacific Ocean. The following are characteristics of this area:

1) The Kanto plain, which is roughly 100x100 km, is the largest plain in Japan and is not limited by a mountainous area except on the north and west sides. 2) The plain includes the Tokyo metropolitan area, which is heavily urbanized and the busiest airspace area. Wind shear detection associated with internal gravity waves would be required the most in this area. This climatology will be of relevance for future studies on aviation safety.

Internal gravity wave events were basically manually identified from Doppler velocity images. Microburst alert information caused by strong divergent pattern associated with gravity waves were also referred. During the study period(1998-2003), six internal gravity waves were identified from the Narita DRAW.

3. WAVE CHARACTERISTICS

a. Occurrence frequency

Table 1 summarizes the characteristics of the internal gravity waves. Figure 2 represent a PPI scan of the Doppler velocity near the surface (the lowest elevation is 0.8) of the Narita DRAW at 1728 JST on 15 January 1998. Figure 3 indicates the occurrence frequency of internal gravity waves during the study period. The frequency of internal gravity waves is concentrated during the cold season (October-January) and is maximal for January.

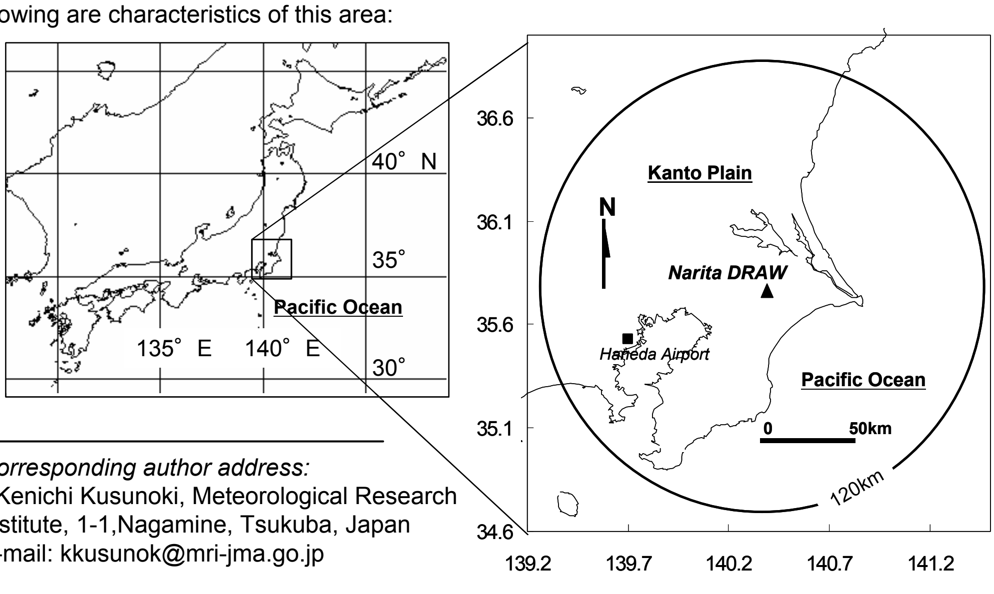

Fig. 1 Map showing the study area. The triangle indicates the position of the Narita DRAW and the Narita International Airport. The squire indicates the position of the Haneda International Airport.

Corresponding author address:
* Kenichi Kusunoki, Meteorological Research Institute, 1-1,Nagamine, Tsukuba, Japan
E-mail: kkusunok@mri-jma.go.jp

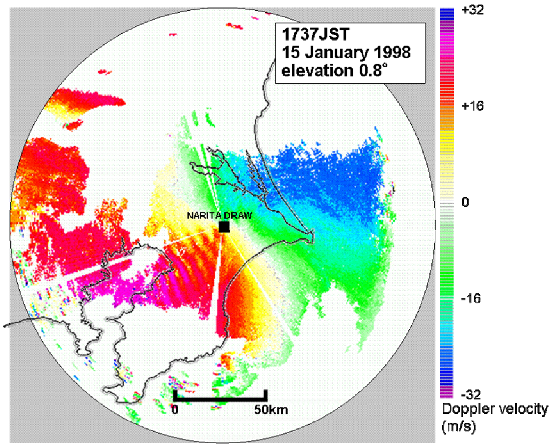

Fig. 2. Typical PPI scan of clear-air echo reflectivity from the Narita DRAW at an elevation angle of 0.8 at 1728 JST on 15 January 1998 (north toward top of page). Positive (negative) velocity means receding from (approaching) the radar.

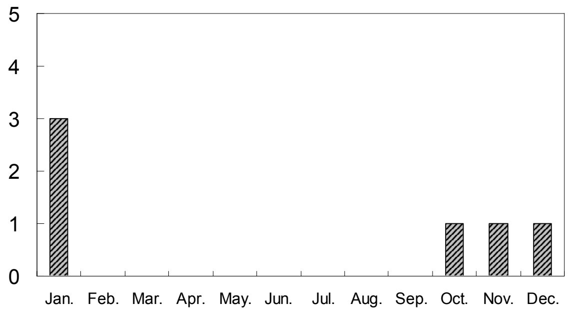

Fig. 3. Monthly distribution of occurrence frequency of internal gravity waves from January 1998 to July 2003.

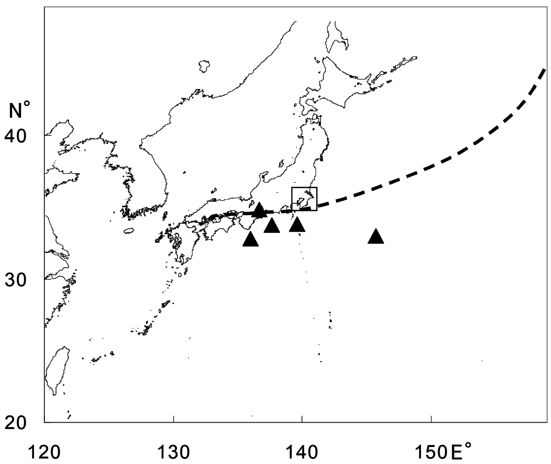

Fig. 4 The locations of the centers of cyclones (triangles) and the stationary front (a dashed line) associated with internal gravity waves over the Kanto Plain (1998-2003).

b. Type of synoptic surface weather patterns

Two synoptic surface weather patterns were identified associated with internal gravity waves over the Kanto Plain. All but one of the 6 surface weather patterns were coastal cyclones. The centers of these cyclones (triangles in Fig. 4) were located off the southern coast of Honshu Island, Japan. The other one was associated with a stationary front (a dashed line in Fig. 4).

c. Horizontal and vertical wavelength

Doppler velocity near-surface (the lowest elevation is 0.8) patterns are shown in Fig. 5. The vertical profiles of variables of Doppler velocities at particular phases (i.e., troughs and ridges) at the waves are shown in Fig. 6. As a characteristic feature of the vertical structure of the waves, these waves have nodes and loops. The most prominent example is seen for the case of 15 October 1998. There were three nodes (i.e., around 500m AGL, around 1500m AGL, and around 2000m AGL) and three loops (i.e., at the surface, around 1000m AGL, around 1800m AGL , and around 2200m AGL). Figure 7 plots the horizontal and vertical wavelength data. The horizontal wavelength ranged from 4.5 to 7.0km while the vertical wavelength ranged from 1.2 to 4.3km.

d. Phase vectors

Figure 8 shows the ground relative phase speed and the direction of propagation of the waves. The phase speeds ranged from 1.0 to 9.0ms^{-1}. The wave directions ranged from 30deg to 75deg.

e. Horizontal velocity amplitudes

Figure 9 shows the maximum amplitude of perturbation horizontal velocities as a functions of height. The maximum velocity amplitude is near the ground, typically about 100m, with maximum of 18ms^{-1}. In Fig. 10, the data from Fig. 9 are replotted as maximum horizontal divergences. This figure indicates that all the events occurred with a wind shear greater than the warning threshold commonly accepted in aviation safety [i.e., 2.5$ms^{-1}km^{-1}$ (Wilson et al. 1984)].

4. CLONLUSIONS

From 1998 to 2003, six events of internal gravity waves were observed with the Narita DRAW. All the events occurred during the cold season, i.e. from October to January. It is noteworthy that all the events occurred with a wind shear greater than the warning threshold commonly accepted in aviation safety. While the wind shear detection algorithms of DRAW have been tuned to recognize microbursts and gust fronts, new algorithms would have to be developed for gravity waves.

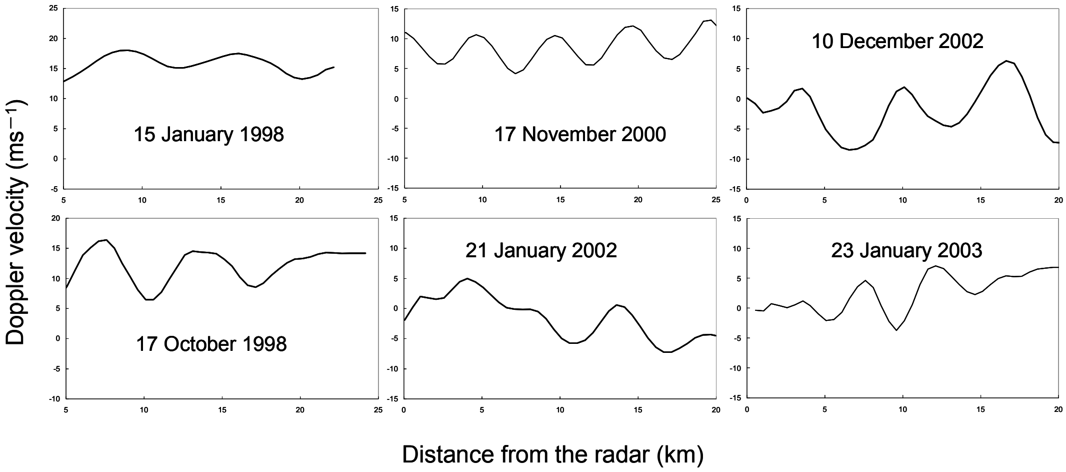

Fig. 5. Doppler velocity near-surface (the lowest elevation is 0.8) patterns.

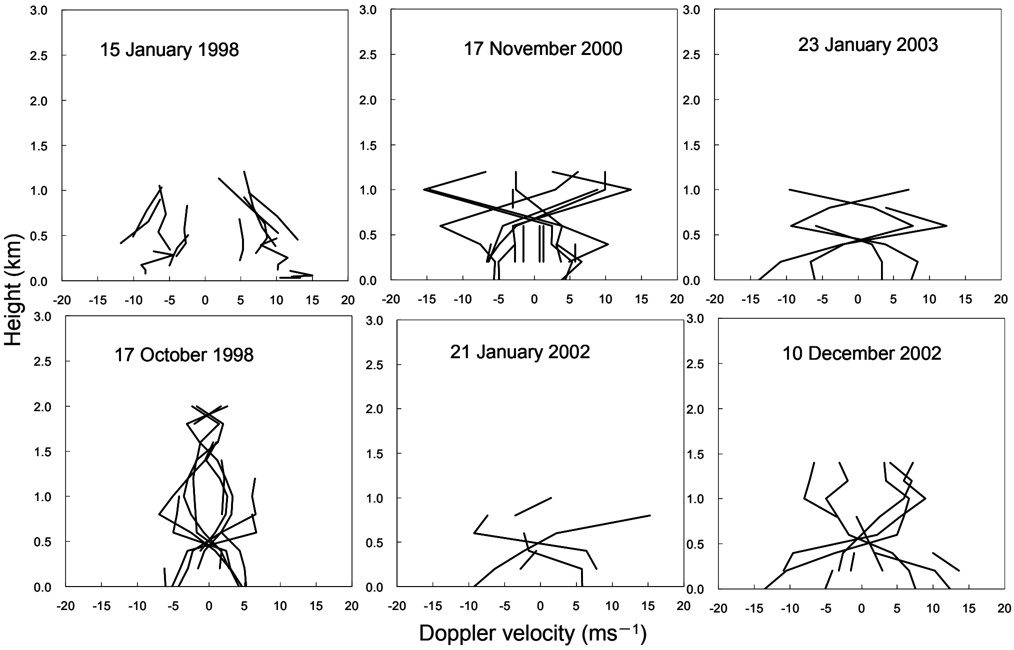

Fig. 6. The vertical profiles of variables of Doppler velocities at particular phases (i.e., troughs and ridges) at the waves.

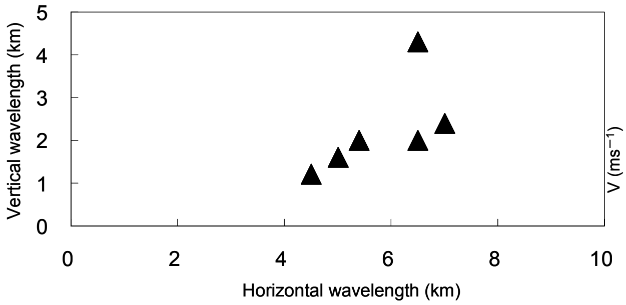

Fig. 7. Plots of horizontal and vertical wavelength.

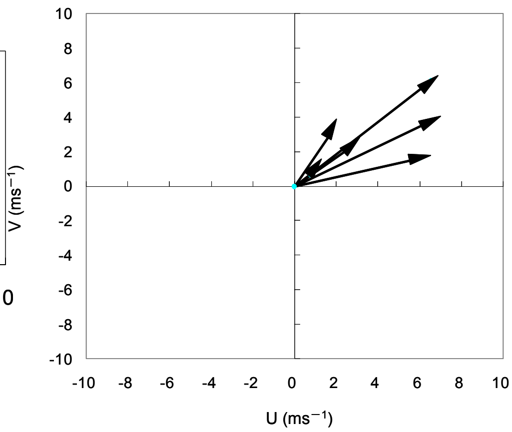

Fig. 8. Phase vectors of the waves.

REFERENCES

Kusunoki, K. and H. Eito., 2003: Analytical studies of low-level internal gravity waves over the Kanto Plain associated with a stationary front. *Mon. Wea. Rev.*, **131**, 236-248.

Miller, D.W., 1999: Thunderstorm induced gravity waves as a potential hazard to commercial aircraft. Preprints, *8th Conf. on Aviation, Range and Aerospace Meteorology*, Amer. Meteo. Soc., 225-229.

Wilson, J. W., R. D. Roberts, C. Kessinger, and J. McCarthy., 1984: Microburst wind structure and evaluation of Doppler radar for airport wind shear detection. *J. Climate Appl. Meteor.*, **23**, 898-915.

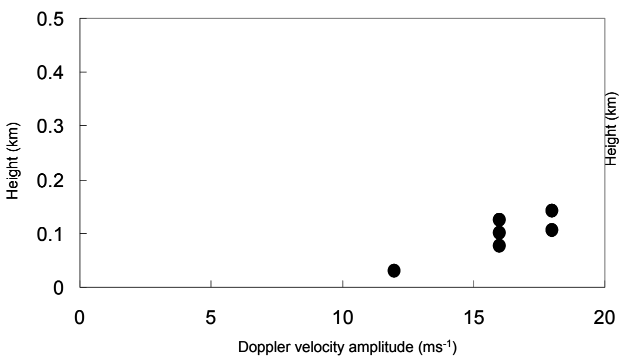

Fig. 9. Maximum amplitude of perturbation horizontal velocities, versus height at the maximum amplitude.

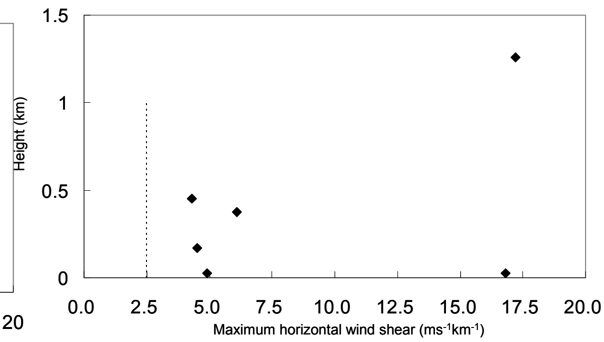

Fig. 10. Maximum horizontal divergences versus height. The vertical dotted line indicates the warning threshold commonly accepted in aviation safety.

Date	15-Jan-98	17-Oct-98	17-Nov-00	21-Jan-02	10-Dec-02	23-Jan-03
Wave period (min.)	30.0	117.0	25.0	13.0	15.0	8.0
Horizontal phase speed (ms^{-1})	3.5	1.0	3.5	6.2	7.0	9.0
Direction of wave motion (degree)	50.0	50.0	30.0	75.0	60.0	47.0
Horizontal wavelength (km)	6.5	7.0	5.4	5.0	6.5	4.5
Vertical wavelength (km)	4.3†	2.0	2.0	1.6	2.0	1.2
Maximum horizontal wind shear (ms-1km-1) / Height (m)	4.3 /454.0	6.1 /374.9	4.5 /167.0	4.9 /25.8	17.2 /1256.0	16.8 /23.2
Maximum horizontal velocity amplitude (ms^{-1}) / Height (m)	12.0 /31.0	15.7 /165.0	16.0 /102.0	16.0 /126.0	18.0 /142.0	18.0 /106.0
Wave observation period (hour)	1.0	0.7	0.5	0.5	1.2	4.0
Surface pressure perturbation amplitude (hPa)	1.0	1.0	0.8	0.9	0.9	0.6
Synoptic pattern	CC*	SF**	CC	CC	CC	CC

†calculated from linear theory * Coastal cyclone ** Stationary front

Table 1. Summary of the characteristics of the internal gravity waves from 1998 to 2003.